SCA2003-31: ADVANCES IN RESISTIVITY MEASUREMENTS USING THE FRIM METHOD AT RESERVOIR CONDITIONS. APPLICATIONS TO CARBONATES.

M. FLEURY
Institut Français du Pétrole

This paper was prepared for presentation at the International Symposium of the Society of Core Analysts held in Pau, France, 21-24 September 2003

ABSTRACT

The Fast Resistivity Index Measurement (FRIM) method is a recent technique to measure continuous resistivity index curves on core samples. In a previous paper of the same author, it has been validated extensively using numerical simulations and experiments performed at ambient conditions. This paper presents the use of this technique at reservoir conditions during drainage and imbibition on various reservoir carbonate samples. The appropriate experimental procedures are presented in order to obtain RI curves representative of field conditions and free of artifacts. We present also two semi-empirical RI-Sw relationships useful for describing the various non-Archie curves observed.

INTRODUCTION

Oil in place is essentially estimated using resistivity logs. Fortunately, the resistivity measurement is very sensitive to the water saturation at low values and a high contrast exists between a formation saturated at 100% and a formation at connate water saturation. However, the relationship between resistivity and saturation must be calibrated in order to have reasonable uncertainties. This is particularly true in carbonates for which the default Archie law $RI=R(Sw)/R(Sw=100\%)=Sw^{-2}$ is rarely verified. The second use of resistivity is the estimation of water flooding efficiency in mature reservoir, which needs the RI-Sw relationship in imbibition.

In the laboratory, the best and quicker way to establish this relationship has been a matter of research for the past ten years. Resistivity measurements are apparently simple to perform and instruments always give a response. However, there are multiple sources of possible artifacts. In addition, it is now recognized that RI(Sw) relationships in carbonates can be quite complex; not only the n value can vary in a wide range (1.5 – 2.5), but also it can vary as a function of saturation, i.e. RI(Sw) is non linear in log-log scale.

We summarize first the essential aspects of the FRIM method. Then we describe the experimental set-up build for reservoir conditions and discuss the impact of non-uniform saturation profiles on the measured RI curves. Based on experimental data, we propose two relationships useful to model the various non-Archie curves measured at reservoir conditions on carbonate samples.

SUMMARY OF THE FRIM METHOD

The Fast Resistivity Index Measurement (FRIM) method is a recent technique developed by the same author in order to circumvent the major draw-back of the standard technique relying on capillary pressure equilibrium that are difficult and time consuming to reach. It was conceived originally in the context of new designs aiming at reducing the experimental time of capillary pressure experiments by (i) reducing the sample length and (ii) using thin semi-permeable membranes with smaller pressure drop than ceramic (Longeron et al. 1995, Fleury and Longeron, 1996). With the same objective in mind, Zeelenberg and Schipper (1991) proposed earlier the continuous injection (CI) technique, a different operational mode of the standard design (ring electrodes/porous plate).

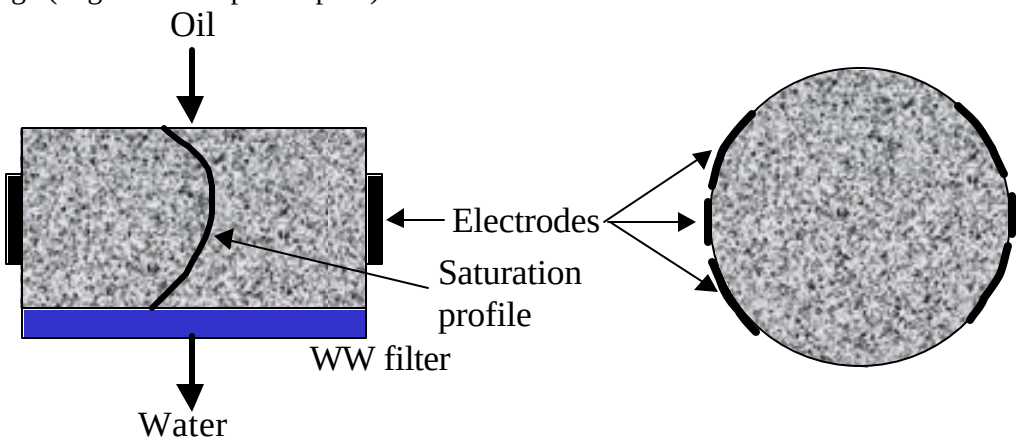

Figure 1: Schematic of electrodes and flow injection in the FRIM method (drainage mode). The large electrodes are used to inject the current, the small ones are used to measure the voltage. The shape of the saturation profile between capillary equilibrium states when injecting oil is indicated qualitatively.

The key aspect of the method lies in the radial electrode geometry design (Figure 1). The current is injected using four large electrodes connected by pairs and the voltage drop using two smaller electrodes located in between. In this geometry, the electrical field is relatively uniform in a horizontal plane (Figure 2, left); in a vertical plane (Figure 2, right), it is more complex and depends (weakly) on the conductivity of the liquid or the end-piece present at the faces of the sample, as discussed later. As described in Fleury (1998), when oil is injected at one face, a saturation front will developed across the sample. If the saturation profile at a given time is Sw(z), the average resistance <R> measured can be considered in parallel with respect to Sw(z), that is:

$$< R >= \left[< \frac{1}{R_0 Sw(z)^{-n}} > \right]^{-1} \qquad (1)$$

where we took for convenience an Archie law with a saturation exponent n for linking resistivity to saturation (Ro is the saturation at Sw=1). When measuring only average saturation and resistance, we deduce nd from the data using $<R>=Ro<Sw>^{-nd}$.

The true n and the measured nd are strictly equal when the saturation is uniform (capillary equilibrium) or when n=1, which is not a realistic value.

When n=2, a typical value for clean sandstones, the effect of the saturation profile is negligible when (i) the injection of oil is performed in the presence of a semi-permeable filter, either at a fixed pressure or flow rate (ii) the range of saturation is not too large. In the presence of semi-permeable filters, the saturation profile has a semi-circle shape (Figure 1) and is very different from a saturation front developed during a standard flooding (this is considered later for imbibition experiments). This contributes greatly to the insensitivity of the method to the saturation profile. Another argument for keeping semi-permeable filters is that low average saturation can be reached. However, a profile effect could be observed if the saturation changes in the sample are too large, in a similar way as in the continuous injection technique (Maas et al., 2000). Such potential artifacts dictates how the experiment should be operated without the need for additional information such as local saturation measurements or corrections involving unknown parameters (essentially Pc, and Kr curves). The experiment is conducted in a pressure imposed mode using for example three steps to divide roughly the saturation range [Swi , 1] into three intervals (at each step, capillary equilibrium is not needed however). These pressure steps can be deduced from mercury injection curves or by experience. The recommended number of steps is three but we often apply more steps, as shown later.

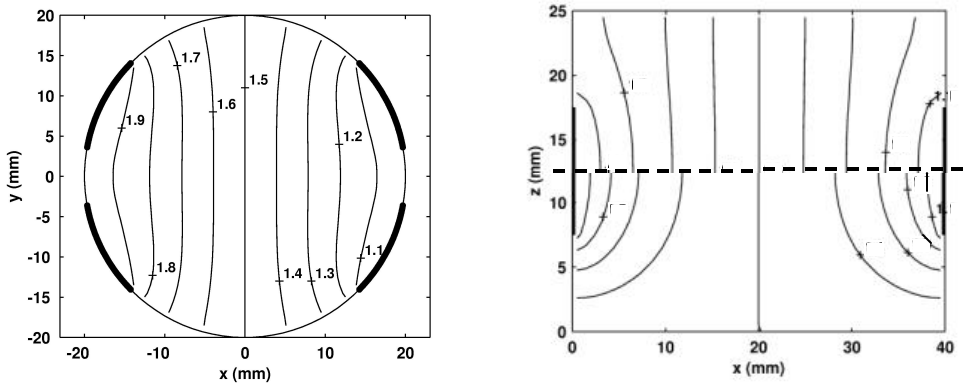

Figure 2: 2D simulations of the electrical field for the radial electrode geometry. The vertical cross-section shows two simulations; for the upper half, a non-conductive end piece or liquid is present at the upper face of the sample where oil is flowing; for the lower half, a conductive end-piece or liquid is present at the lower face of the sample where water is flowing. In the simulation presented, extreme cases of fully conductive and isolating faces are considered, which are extreme cases.

A curve influenced by strong non-uniform profiles is shown schematically in Figure 3. A sudden change in the slope between (pseudo) equilibrium RI-Sw points indicates that the experiment may not be valid. However, even if a single pressure step covering the entire saturation range is applied on a high permeability sample (2400 mD, see figure 4 of Fleury, 1998), the accuracy is still acceptable in the saturation range of practical interest (Sw<0.6).

Therefore, the choice of the pressure steps is not critical. Another example is shown in Figure 4 where a strongly non-linear RI curve is observed. There is no fluctuations of the slope near the 4 capillary equilibrium points shown, and this indicate that the curve is valid and not influenced by non uniform saturation profiles. Such control can be performed in real time by plotting the measured average saturation vs. average resistance. Note that the potential artifacts described above depend also on the pressure drop generated by the semi-permeable filter. Indeed, for a given breakthrough pressure, a high flow rate filter (membranes, composite ceramics) will generate larger saturation changes. Using the procedure described above at ambient conditions, the typical time scale of an experiment is one week. At reservoir conditions, when the sample is originally water-wet, the time-scale of physico-chemical processes occurring during aging must also be taken into account (see next section for further discussion).

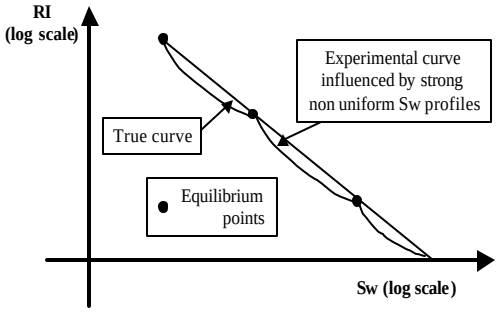

Figure 3: Schematic of RI curves influenced by strong non-uniform saturation profiles.

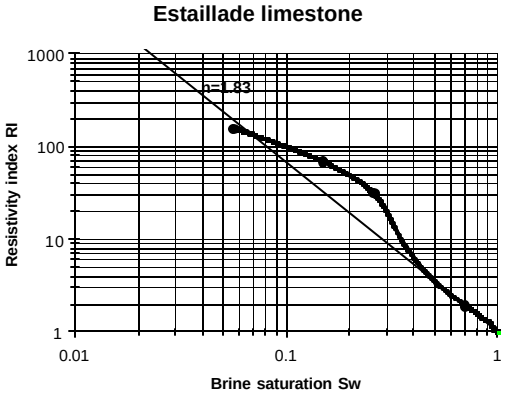

Figure 4: Example of measurement using the FRIM method (double porosity carbonate). No slope fluctuation is seen near the capillary equilibrium points indicated.

The radial electrode design allows the experiment to be quasi-insensitive to saturation profiles. The draw back is that the measured resistance is sensitive to the boundary conditions at the faces of the sample. This is seen on the simulations of the electric field (Figure 2, right): at the upper face, oil is injected, the resistivity is large and the potential lines are mostly perpendicular to the x direction. At the lower face, the ceramic in capillary contact with the sample yield a low resistivity and the potential lines are mostly parallel. In the simulations presented, two extreme cases of conductive and non-conductive boundary conditions have been taken for simplicity. However, the actual resistivity at the faces of the sample is not known accurately due to the presence of metallic parts and the true electric field may be more complex than shown, and their effect on the measured resistance will also depend on the sample resistivity itself. Yet, these effects have no impact of the measurements because (i) the conductivity at the face of the sample are constant during an experiment (ii) the height of the electrodes are limited to about the half of the sample in order to minimize the effects described above. For example, we observe a variation of resistance of a few percent when oil is replaced by water at the upper face.

MEASUREMENTS AT RESERVOIR CONDITIONS

New apparatus running at pseudo-reservoir conditions were build. Based on past experience, the emphasis was put on robustness and high stability rate rather than sophisticated automation which are sources of problems and need high maintenance (the typical experimental time is of the order of weeks making full automation useless).

Drainage RI curves

Drainage RI curves are determined by increasing gradually the oil pressure (Figure 5). Oil pressure is regulated using large gas buffer (not in contact with oil). Resistance are measured at 1 kHz using an isolator (essentially a very high inductance) and an impedance meter and hence, the end-pieces can simply be connected to ground and do not need to be electrically isolated. The electrodes are molded into a Viton sleeve and due to their relatively large surface area, the experiments conducted with overburden pressure may not damage the sample. The ceramic is a 5 mm thick porous alumina with an oil-water entry pressure of 12 Bar (Kw≈0.02 mD). High flux porous plates (Fleury, 1998, Wilson, 2001) could speed-up the experiments but this is not critical. The size of the sample is 30 mm (maximum) in length and 40 mm in diameter (a 50 mm version to increase pore volumes is in progress).

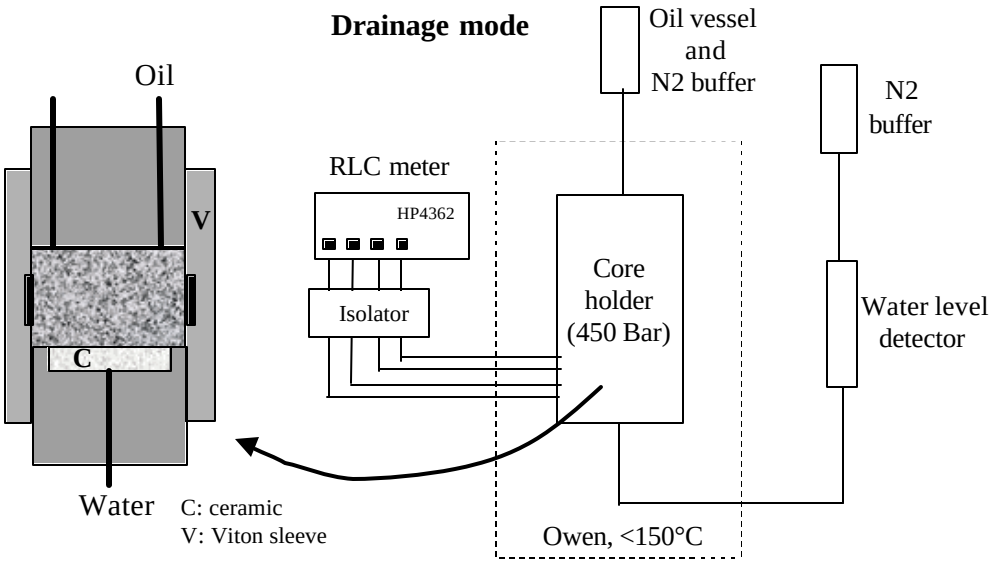

Figure 5: Schematic of the experimental set-up in drainage. The core holder inside the oven can sustain a confining pressure of 450 Bar. The water level detector is maintained at a constant low pressure (<10 Bar).

The measurements shown on Figure 6 show the possible short duration of an experiment (about 10 days). The continuous drainage RI curve obtained is smooth even when saturation and resistance change abruptly, which is an indication that the experiment is properly conducted. In the case presented, the sample was originally cleaned at elevated temperature with strong

solvants and therefore, its wettability was preferentially water-wet at the begining of the experiment. In this case, we applied more than three pressure steps and waited for stable resistance for the purpose of equilibrating the oil/rock surface interactions. Indeed, during drainage by reservoir crude oil, the wettability may be modified and the expected trend is an increase of resistivity compared to the water wet case (in general, resistivity is a very sensitive indicator of fluid redistribution and wettability modification). In the present case, we observe a bending up of the curve at low saturation, triggered by the change of wettability. When this is observed, the time scale for obtaining a stable resistance is increased considerably and an equilibrium may never be reached within practical experimental time. At high saturation, the saturation exponent (1.4) is low compared to standard values. This is further discussed in section Empirical Models for non-Archie Curves where the model used to described the bending up is also presented.

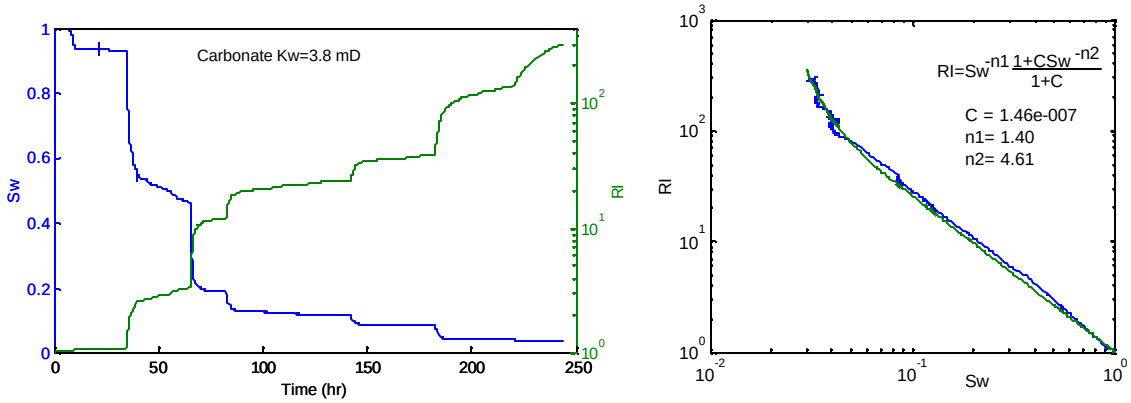

Figure 6: Example of drainage RI curve determined from the measurement of average saturation and resistance (left panel) at reservoir condition (T=115°C, dead oil, net overburden pressure 30 Bar).

Imbibition RI curves

Imbibition RI curves are measured during spontaneous and forced imbibition displacements. To obtain the spontaneous part, the oil pressure is gradually decreased down to the water pressure at the end of drainage. Then, the set-up is switch to the forced imbibition mode as shown in Figure 7. For practical reasons, we propose to measure the forced-imbibition RI curves without using oil-wet semi-permeable filters (i.e. inject water at a higher pressure in Figure 1 and use an oil-wet semi-permeable filter at the upper face) although this method is the most accurate one. Instead, water is injected through the ceramic at very low (0.1 cc/h, about 0.01 PV/hr for a 30% porosity sample) to low flow rate (1-10 cc/hr). At the outlet face, the produced oil is swept at high flow rate
(100-500 cc/h) in order to synchronize the saturation and resistivity measurements and to minimize oil trapping in the tubings and valves. An intermediate mode can also be used to accelerate the spontaneous imbibition by keeping the drainage level detector connected and sweeping the outlet face at the same time. In terms of saturation profiles, we are in this case in a

very different situation and we performed a numerical study to evaluate the impact of saturation profiles on the RI measurements.

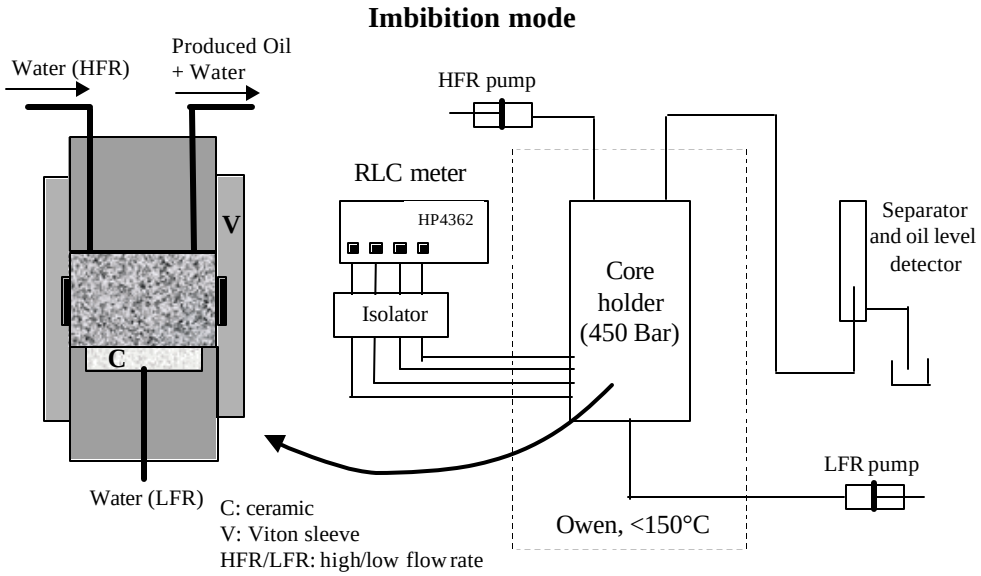

Figure 7: Experimental set-up in imbibition. Water is injected at very low flow rate (LFR) through the ceramic. At the inlet face, a spiral allows the produced oil to be collected and measured quickly outside the oven without significant delay compared to the resistance.

Effect of saturation profiles

During water flooding, the saturation profiles have a typical shape as shown in Figure 8 (left panel). They were obtained by numerical simulations for a typical oil-wet system (Pc: small negative entry pressure, dPc/dSw(Sw=50%) of about 0.005 Bar/%, oil-water Corey exponent set respectively to 4 and 3). Then, for each profile, we calculated the series Rs and parallel Rp resistance according to:

$$Rs=<R(z)> = Ro /<Sw(z)^{-n}> \qquad Rp = 1/<1/R(z)> = Ro<Sw(z)^{n}> \qquad (2)$$

with n=2. Rp represents the radial electrode geometry measurement, Rs represents the standard ring electrode measurement. For Rs, the distance between the electrodes was set to ¾ of the sample length (the results presented here are not dependant of the actual length). Then, Rs and Rp are plotted versus average saturation and compared to the true value (Figure 8, right panel). Clearly, the standard ring design is very sensitive to the profiles, as described by Maas et al. (2000). The radial electrode design is much less sensitive and the measured curve underestimates slightly the true resistivity curve. This effect will be minimized if the experiment is conducted with successively very low, low and medium injection flow rates. In these situations, the saturation range covered for each flow rate is limited (Figure 8, left panel) and the profiles have a weaker effect. The measured imbibition curve is not as accurate as in drainage but the experiment has a

short duration of about 2-3 days, is simple to operate and covers the saturation range of practical interest.

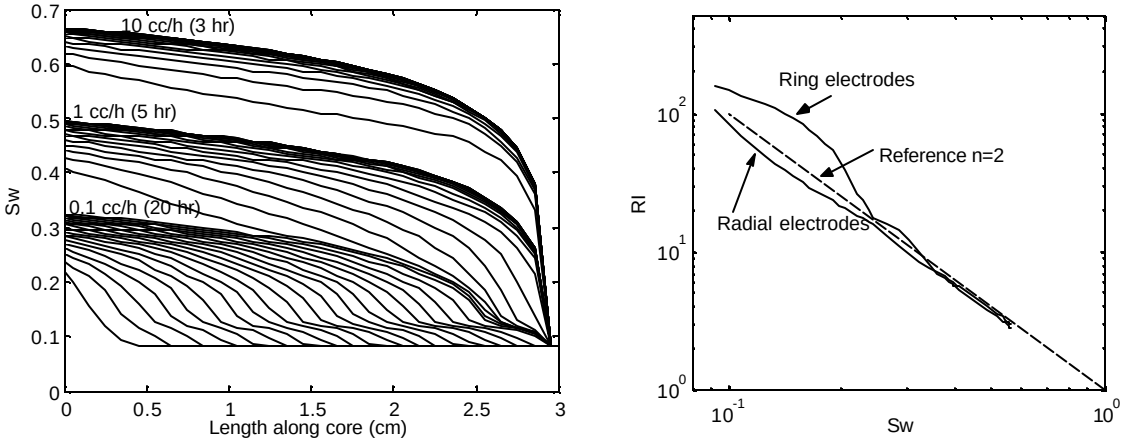

Figure 8: An example of the effect of saturation profiles on RI curves during imbibition. For comparison, the calculation using the standard method is also shown (ring electrodes spanning over ¾ of the sample length). The duration of each injection period is indicated in parentheses.

An example of measurement of a drainage-forced imbibition cycle is shown in Figure 9. The drainage RI curve can be accurately modeled by an Archie law. However, the imbibition shows a severe hysteresis associated with wettability effects. In this experiment, a sequence of very low to medium flow rate was applied as described above. There is no ambiguity about the existence of this hysteresis because the imbibition RI values are at worst underestimated.

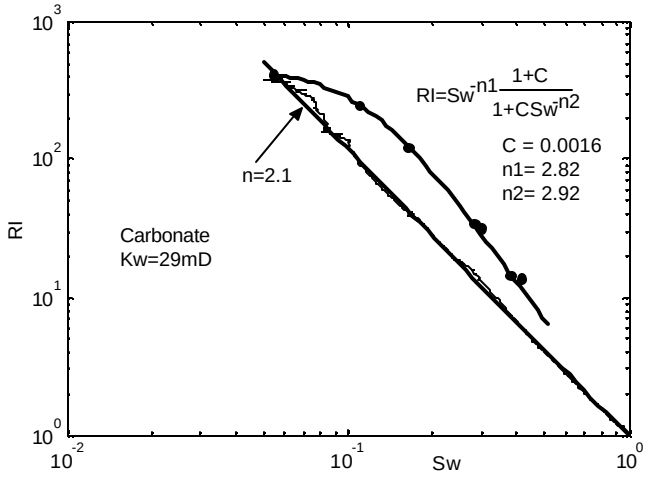

Figure 9: Example of measurement of drainage - forced imbibition RI curves. Reservoir conditions, dead oil.

EMPIRICAL MODELS FOR NON-ARCHIE CURVES

The measurements can often not be described by simple Archie's law. We propose two semi-empirical models for bending up and down curves (Figure 10). For bending down curves, the data are fitted using three parameters n_1, n_2 and C according to:

$$RI = Sw^{-n1}\frac{1+C}{1+CSw^{-n2}} \tag{3}$$

When C=0, equation 2 reduces to an Archie law. The exponent n_1 is the slope at Sw=1. This model can describe drainage RI curves flattening at low saturation. In the case of the primary drainage of double porosity water-wet porous media, C can be interpreted as the conductivity ratio of the two pore populations acting in parallel (Fleury, 2002). In this work, this relationship is also used to describe imbibition curves (Figure 9, Figure 11, in the example shown, only a few data points are available on the imbibition curve because the data acquisition system was not completed at the time of the experiments). It proved to be adequate in many cases (more than shown in this paper) although the physical mechanisms producing this strong hysteresis is clearly linked to the oil-water distribution in the porous space and not to its structure. The implication for log calibration is quite important; if one uses the drainage curve to calibrate resistivity in a water flooded zone, the saturation may be underestimated by about 20 saturation units.

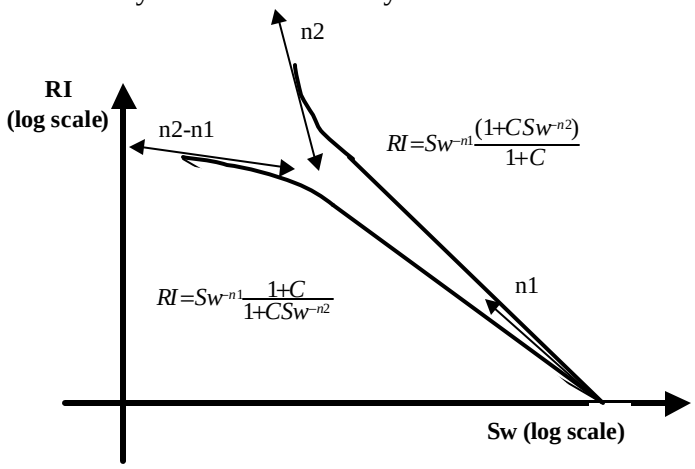

Figure 10: Semi-empirical RI(Sw) relationship proposed to describe the measurements. The slope at low saturation is n_2-n_1 and n_2 for the bending down and bending up curves respectively.

For RI curves bending up at low saturation, we used the following empirical formula:

$$RI = Sw^{-n1}\frac{(1+CSw^{-n2})}{1+C} \tag{4}$$

Similarly, this formulation reduces to an Archie law for C=0. For this equation, the slope near Sw=1 is n_1 and the slope at low saturation is n_2, in log-log scale (Figure 10). Two examples are shown (Figure 6, Figure 12) where the wettability produces such shape.

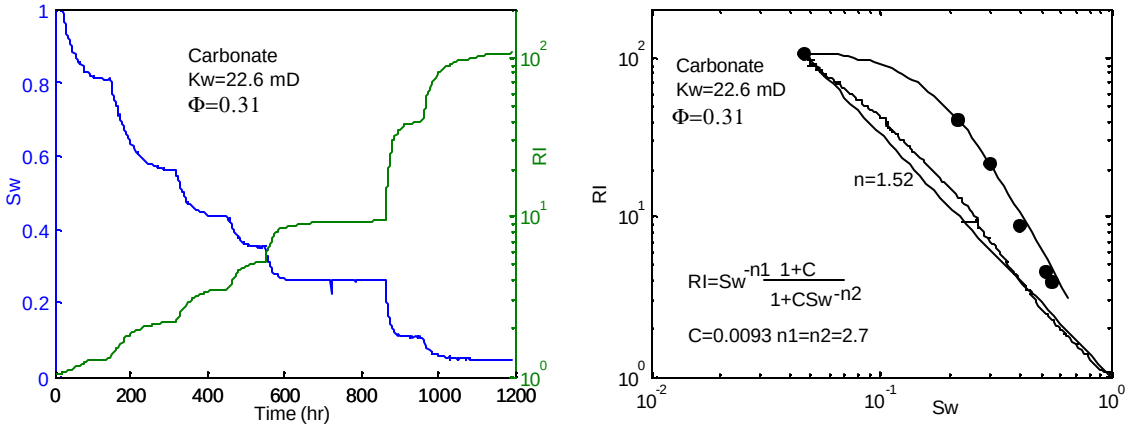

Figure 11: Example of the model for fitting curves bending down at low saturation.

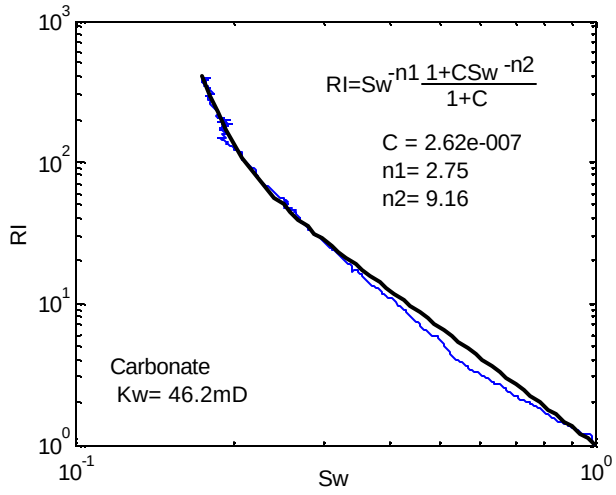

Figure 12: Example of curve bending upward under the effect of wettability.

DISCUSSION

In carbonates, we observe a large variability of RI curves. In a relatively small set of samples, one can find at reservoir conditions low n values (1.5, Figure 11, initial slope of 1.4 in Figure 6) and high n values (2.75, Figure 12) with bending up curves. In this case, the samples studied can be considered as homogeneous (as indicated by X-ray CT scans) and are not very

different in terms of mineralogy (calcite is dominant). In addition, the low n value was obtained despite a very long experiment (about 50 days, Figure 11, left panel) in which oil-rock surface interaction can occur and stabilize. For this sample, a low n value and a linear log-log RI curve in drainage strongly suggest a water-wetness. However, the strong hysteresis in imbibition suggest on the opposite an oil-wettness. Indeed, it is generally accepted that water wet sample do not exhibit RI drainage-imbibition hysteresis and this is confirmed by our own past and present experience where we compared RI curves at ambient and reservoir conditions (not shown, however bimodal water-wet pore structure can exhibit an hysteresis not linked to wettability). In practice, the large fluctuations from one sample to the other generate large uncertainties in log calibration.

CONCLUSIONS

We have shown the use of the Fast Resistivity Index Measurement (FRIM) method at reservoir conditions in drainage and imbibition. In drainage, there is little change compared to the ambient conditions described earlier, except that the kinetics of physico-chemical processes must be taken into account. During spontaneous imbibition, the procedure is similar to drainage. During forced imbibition, the RI curve is determined during a water flooding and a careful choice of flow rate must be made to avoid underestimation of resistance. The proposed water flooding procedure is a good compromise between speed and accuracy. At reservoir conditions, the change of wettability produces non-Archie behaviors either in drainage or in imbibition. We propose two empirical formulations greatly simplifying the data analysis. In carbonates, we also observe large fluctuations of the saturation exponent (1.4 – 2.7) in saturation ranges where Archie models apply.

ACKNOWLEDGMENTS

The author wishes to acknowledge P. Poulain and G. Thibault for performing the experiments. The simulations were performed using CYDAR, a software designed by R. Lenormand.

REFERENCES

Fleury M. and D. Longeron, 1996, "Combined resistivity and capillary pressure measurements using micropore membrane technique", Proceeding of the International Symposium of the Society of Core Analysts, Montpellier.

Fleury M, 1997, Apparatus having semi-permeable membranes for testing geological samples, Patent N° EP98400771.

Fleury M., 1998, "FRIM: a new method for measuring continuous resistivity index curves", Proceeding of the International Symposium of the Society of Core Analysts, Den-Hague, 14-16 September.

Fleury M., 2002, "Resistivity in carbonates: new insights", Proceeding of the International Symposium of the Society of Core Analysts, Monterey, 22-25 September.

Wilson Ove Bjørn, Bjørn Gunnar Tjetland and Arne Skauge, 'Porous plate influence on effective drainage rates in capillary pressure experiments', Proceeding of the International Symposium of the Society of Core Analysts, Abu Dhabi, Edingburgh, September 2000.

Longeron D., W.L. Hammervold and S.M. Skjaeveland, 1995, "Water-Oil Capillary Pressure and Wettability Measurements Using Micropore Membrane Technique" , paper SPE 30006 presented at the International Meeting on Petroleum Engineering in Beijing, PR China, 14-17 November.

Maas J.G., N. van der Post, Krijn H., van der Gyp, John G.C. Coenen and W. J. Looyestijn, Resistivity index measurements under weak capillary forces. Proceeding of the International Symposium of the Society of Core Analysts, Abu Dhabi, September 2000.

Zeelenberg H.P.W. and Schipper B.A., Developments in I-Sw measurements, in Advances in Core Evaluation II, Reservoir Appraisal, Gordon and Beach Science Publishers, Philadelphia, p. 257, 1991.

Wilson Ove Bjørn, Bjørn Gunnar Tjetland and Arne Skauge, 'Porous plate influence on effective drainage rates in capillary pressure experiments', Proceeding of the International Symposium of the Society of Core Analysts, Abu Dhabi, Edingburgh, September 2000.